Published in final edited form as:
Curr Biol. 2012 March 20; 22(6): 451–460. doi:10.1016/j.cub.2012.01.060.

ENDOCYTOSIS GENES FACILITATE PROTEIN AND MEMBRANE TRANSPORT IN *C. ELEGANS* SENSORY CILIA

Oktay I. Kaplan[1,*], **David B. Doroquez**[2,*], **Sebiha Cevik**[1], **Rachel V. Bowie**[1], **Lara Clarke**[1], **Anna A.W.M. Sanders**[1], **Katarzyna Kida**[1], **Joshua Z. Rappoport**[3], **Piali Sengupta**[2,^], and **Oliver E. Blacque**[1,^]

[1]School of Biomolecular and Biomedical Science, UCD Conway Institute, University College Dublin, Belfield, Dublin 4, Ireland [2]Department of Biology and National Center for Behavioral Genomics, Brandeis University, Waltham, MA 02454, USA [3]School of Biosciences, College of Life and Environmental Sciences, University of Birmingham, Birmingham, UK

SUMMARY

Background—Multiple intracellular transport pathways drive the formation, maintenance and function of cilia, a compartmentalised organelle associated with motility, chemo-/mechano-/photo-sensation, and developmental signaling. These pathways include cilium-based intraflagellar transport (IFT) and poorly understood membrane trafficking events. Defects in ciliary transport contribute to the aetiology of human ciliary disease such as Bardet-Biedl syndrome (BBS). In this study, we employ the genetically tractable nematode *Caenorhabditis elegans* to investigate if endocytosis genes function in cilium formation and/or the transport of ciliary membrane or ciliary proteins.

Results—Here we show that localisation of the clathrin light chain, AP-2 clathrin adaptor, dynamin and RAB-5 endocytic proteins overlaps with a morphologically discrete periciliary membrane compartment associated with sensory cilia. In addition, ciliary transmembrane proteins such as G protein-coupled receptors concentrate at periciliary membranes. Disruption of endocytic gene function causes expansion of ciliary and/or periciliary membranes as well as defects in the ciliary targeting and/or transport dynamics of ciliary transmembrane and IFT proteins. Finally, genetic analyses reveal that the ciliary membrane expansions in dynamin and AP-2 mutants require *bbs-8* and *rab-8* function, and that sensory signaling and endocytic genes may function in a common pathway to regulate ciliary membrane volume.

Conclusions—These data implicate *C. elegans* endocytosis proteins localized at the ciliary base in regulating ciliary and periciliary membrane volume, and suggest that membrane retrieval from these compartments is counter-balanced by BBS-8 and RAB-8-mediated membrane delivery.

INTRODUCTION

Cilia extend most eukaryotic cell surfaces and are essential for cell/fluid motility, chemo-/mechano-/photo- sensation and developmental signalling [1]. Malformation or dysfunction

^Correspondence to: oliver.blacque@ucd.ie or sengupta@brandeis.edu, Tel: +353-1-7166953, Fax: +353-1-2837211.
*These authors contributed equally to this work

of cilia underlies numerous diseases and multi-symptomatic disorders such as polycystic kidney disease, *retinitis pigmentosa* and Bardet-Biedl syndrome (BBS) [2].

Canonical cilia possess nine doublet microtubules extending from a plasma membrane-anchored basal body centriole. Ciliary morphologies are diverse with varying branch numbers as in mammalian olfactory cilia, or an extended membrane compartment as in the photoreceptor outer segment [3]. Ciliary membranes house transmembrane signalling molecules required for sensory transduction or developmental signalling [1]. Correct ciliary function requires localisation of ciliary molecules to appropriate ciliary subdomains, and restricting access of non-ciliary proteins [4]. The ciliary base contains important evolutionarily conserved features that compartmentalise the organelle by providing structural and diffusion blocks to transport [4]. These include the transitional fibers connecting the distal end of the centriole to the plasma membrane, thus defining the ciliary-periciliary membrane junction and restricting vesicle entry into cilia. Further blocks are provided by the ~1 μm long transition zone, immediately distal to transitional fibers [5].

As cilia lack protein synthesis, proteins must be trafficked to the organelle. The best understood delivery system is intraflagellar transport (IFT), a conserved non-vesicular, bidirectional motility along ciliary axonemes essential for cilium biogenesis and function [6]. In addition, cilium formation and transport employs membrane trafficking machineries and regulators including secretory/exocytic components such as the AP-1 clathrin adaptor, Arf4, Rab8, Rabin8 and the exocyst complex [7–15]. Many of these components dock at the ciliary base proximal to the transition zone and mediate ciliary protein transport via vesicular fusion and trafficking within cilia.

Although roles for exocytosis in regulating ciliary protein transport and composition have been described, similar roles for endocytic events at the ciliary base are not well understood. Clathrin coated pits are found at ciliary/flagellar pockets in mammalian cells and unicellular protists [16, 17]; these pits are active and dynamic, capable of mediating transferrin endocytosis [17]. Furthermore, endosome-associated proteins STAM-1, HGRS-1 and RAB-5 localise beneath *C. elegans* male sensory cilia and regulate the ciliary localisation and signalling of polycystin complexes [18]. However, whether endocytosis plays a general and widespread role in regulating cilia structure and function remains unclear.

Here we examine whether endocytosis-associated genes define the nematode ciliary compartment. In *C. elegans*, cilia extend from distal dendrite tips of 60 highly polarized sensory neurons, house sensory signalling molecules, and enable worms to sense environmental stimuli [19]. We show that pools of endocytic proteins are found immediately proximal to sensory cilia, overlapping with a morphologically distinct compartment we call the periciliary membrane compartment (PCMC). Disruption of endocytic gene function causes expansions of periciliary and ciliary membranes and defects in ciliary protein localisation and transport in specific cell types. Furthermore, ciliary membrane and PCMC expansions require *bbs-8* and *rab-8* function, suggesting that maintenance of PCMC and ciliary membranes requires regulated membrane delivery via BBS-8 and RAB-8 exocytic mechanisms counter-balanced by membrane retrieval via endocytic proteins.

RESULTS

Endocytic proteins are enriched in a periciliary membrane compartment

To determine whether endocytic components are associated with cilia, we examined the subcellular localisation of GFP-tagged components of the clathrin-mediated endocytosis pathway in ciliated sensory neurons. Proteins examined included CLIC-1 clathrin light chain, DPY-23 AP-2 adaptor μ2 subunit, early endosome component RAB-5 and DYN-1

dynamin. Co-expression of full-length GFP-tagged endocytic proteins with mCherry-tagged CHE-13 (IFT57) that labels all sensory cilia in amphid (head) and phasmid (tail) sensory organs showed punctate GFP localisation in the far distal dendrite region, immediately proximal to cilia (Figure 1A; Figure S1A). The distal extent of these endocytic protein pools overlapped with the CHE-13 pool at the ciliary base (Figure 1B). These IFT pools correspond to the transitional fiber region below ciliary transition zones and thus precisely mark the junction between dendritic and ciliary compartments [5]. In agreement with endocytic proteins participating in dynamic transport functions at the ciliary base, GFP::RAB-5 fusion protein molecules, presumably associated with vesicles, frequently emerge from the far distal dendrite pools and translocate along dendrites towards the soma (Figure S1B; Movie 1). Such motility was not observed for CLIC-1 or DPY-23. Although enrichment of endocytic proteins at the base of cilia was consistently observed, we also found signals in other parts of the cell including atpresynaptic zones (Figure S1A).

The far distal dendrite region enriched for tagged endocytic proteins appeared as an ~0.5 μm^2 bulge (Figure 1A–C), suggesting this dendritic region may define a morphologically distinct compartment. Using transmission electron microscopy (TEM) on longitudinal sections from wild type (WT) cilia, we found that the dendrite region immediately proximal to transition zones (TZ) was indeed bulge-like and demarcated at its proximal side by electron dense belt-shaped junctions between the ciliated cell and the surrounding glial support cell (Figure 1D, E; Figure S1C). These compartments frequently contained vesicles, typically 30–120 nm diameter (Figure 1E; Figure S1C) some of which appeared to be coated (arrow in Figure 1E; Figure S1C). Together, these data indicate that a pool of endocytosis-associated components exists at the ciliary base of nematodes, overlapping with a morphologically distinct, vesicle-containing compartment that we hereafter call the *C. elegans* periciliary membrane compartment (PCMC) (Figure 1F). These conclusions are consistent with endosomal RAB-5, STAM-1 and HGRS-1 localising at the base of male sensory cilia and with observations showing vesicles beneath the ciliary TZs of *C. elegans* sensory neurons [9, 18].

We also found a highly enriched pool of clathrin at the base of flagella in *Chlamydomonas* green algae and in mouse sperm cells (Figure 1G, Figure S1D, E). Thus, together with previous reports of clathrin localisation beneath cilia/flagella in unicellular *Trypanosoma* and *Tetrahymena* [17, 20–22], it appears that ciliary base enrichment of endocytic components is a conserved feature in multiple species.

Endocytic genes regulate ciliary and PCMC morphology in different cilia types

We next investigated the roles of endocytic genes *dpy-23*, *dyn-1*, and *rab-5* in defining the nematode cilium and/or the PCMC. Two alleles of *dpy-23* were used, *e840* (large deletion and, hence, likely a null mutation) and *gm17* (splice site mutation), both of which reduce, but do not abrogate, AP-2 complex formation. [23]. As null mutations in *dyn-1* and *rab-5* result in embryonic or early larval lethality, we used the *dyn-1(ky51)* temperature-sensitive allele, or knocked down *rab-5* and *dyn-1* function using cell-specific RNAi [24]. We also investigated the ciliary phenotypes of animals overexpressing *rab-5(Q78L)* and *rab-5(S33N)* transgenes, predicted to encode dominant active (GTP-locked) and inactive (GDP-locked) RAB-5 [25].

Examination of cilium integrity in six pairs of amphid neurons and the PHA/B phasmid neurons by a lipophilic dye uptake assay [26] revealed normal dye-filling responses in *dyn-1* and *rab-5*-disrupted worms (Figure S2A). However, in *dpy-23(e840)* mutants, 40% of PHA/PHB neurons failed to incorporate DiI (Figure S2A). This phenotype was rescued by transgenic expression of *gfp*-tagged *dpy-23(+)* (Figure S2A). Next, we directly visualised cilia using *gfp* markers expressed in ciliated cells that illuminate all sensory neuron

structures. We found that *dpy-23(e840)* worms exhibited truncated PHA/B cilia; however, amphid AWB olfactory and ASER channel cilia were unaffected (Figure 2A). PHA/B and AWB cilia lengths were unaltered in WT worms overexpressing *rab-5(S33N)* and *rab-5(Q78L)* (Figure 2A). Similarly, AWB cilia lengths were normal in *dyn-1(ky51)* mutants and *rab-5* RNAi knockdown animals (Figure 2B).

Although cilia lengths were generally unaffected, the overall morphology of AWB olfactory cilia was markedly altered in all examined gene-disrupted mutants. Compared to the simple rod-like structure of ASER and PHA/B channel cilia, AWB cilia possess two branches, frequently terminating in small membranous expansions (fans) (Figure 2C; bracket). In endocytic gene mutants, a range of different AWB cilium morphologies were observed, grouped into three distinct categories. Category 1 includes cilia resembling those in WT animals with small fans (Figure 2C) [27]. Category 2 includes cilia with abnormally large membrane expansions (either the fans or membrane in more proximal regions of the axoneme) and Category 3 cilia lack one or both branches, or exhibit additional secondary branches (Figure 2C). Mutations in endocytic genes resulted in a marked increase in Category 2 cilia, with smaller changes in the number of Category 3 cilia (Figure 2D). Quantitative measurements of Category 2 cilia revealed only 22% of WT worms with fans $>1\mu m^2$, whereas fans with larger overall area were observed in 30–80% of most endocytic gene-disrupted worms (Figure 2E). Transgenic expression of *dyn-1(+)* rescued both the increased number of AWB cilia with fans and the increased fan area phenotype of *dyn-1* mutants (Figure 2D, E).

Since the localisation of endocytic genes overlaps with the PCMC, we investigated whether PCMC morphologies were altered upon disruption of these genes. Using the ASER and PHA/B GFP markers described above, and an OSM-6 (IFT52) GFP marker [28], PCMC areas were found to be significantly enlarged in *dpy-23* mutants (Figure 2F, G; Figure S2B). The expanded far distal dendrite region corresponds to the PCMC as it lies immediately proximal to the thin rod-shaped cilia that are clearly evident with these markers. Similar PCMC enlargements were also observed using ASK and OLQ ciliary protein markers (see Figure 4 below). Expanded areas were also observed in other regions of *dpy-23* mutant ciliated cells (Figure S2C; arrowheads). TEM analyses of longitudinal sections from *dpy-23* mutant amphid channel cilia confirmed the fluorescence data by showing that the ciliary TZ and belt junction-defined PCMCs were indeed enlarged, containing more periciliary membrane than WT controls (Figure 2H, I; Figure S2D, E). We also found evidence of reduced vesicle number in the *dpy-23* mutant PCMCs (Figure S2E), consistent with reported reduced vesicle number at the neuromuscular synapses of these worms [23]. In contrast, ciliary axonemes were grossly normal with respect to length, morphology and microtubule integrity (data not shown). Together, these findings indicate that although *C. elegans* endocytic genes are not generally required for ciliogenesis, they modulate membrane volume both within AWB cilia and at the PCMC regions of amphid/phasmid channel neurons.

Mutations in bbs-8 and rab-8 genes suppress the expanded ciliary and periciliary membrane phenotypes of endocytic gene mutants

One interpretation of the ciliary membrane phenotypes in endocytic mutants is that membrane components accumulate in cilia or at the PCMC due to defects in endocytic recycling. This hypothesis predicts that disruption of membrane trafficking to cilia would suppress endocytic mutant phenotypes. We found that enlarged AWB cilium fan phenotypes of *dyn-1(ky51)* and *dpy-23(gm17)* mutants were significantly suppressed by *bbs-8(nx77)* loss-of-function mutations, with fans reduced in size and frequency in *dyn-1;bbs-8* and *dpy-23;bbs-8* double mutants, compared with *dyn-1* and *dpy-23* single mutants (Figure 3A). Likewise, *rab-8* mutations also partially suppressed the AWB fan phenotypes of *dyn-1*

mutants (Figure 3A). We also assessed if *bbs-8(nx77)* was required for the enlarged PCMC membrane in *dpy-23(e840*) phasmid neurons and found this phenotype partially suppressed in *dpy-23;bbs-8* double mutants (Figure 3B). Thus, a balance of exocytosis and endocytosis likely regulates ciliary and PCMC membrane volume in individual neurons.

Ciliary proteins are partially mislocalised to different extents in specific cilia types in endocytic gene mutants

Next we asked if endocytic genes facilitate sorting or transport of ciliary membrane or IFT proteins by examining their subcellular localization in specific sensory neuronal subtypes. Proteins examined were the OSM-9 TRPV channel in OLQ cells, the ODR-10 odorant receptor in AWB cells, the SRBC-66 GPCR in ASK cells, and IFT proteins in multiple cilia types, namely OSM-3 (KIF17 kinesin homologue), KAP-1 (kinesin-II subunit), OSM-6 (IFT52; IFT-B protein) and the IFT regulator, BBS-7 (BBSome protein).

In WT OLQ cells, OSM-9::GFP is restricted to the ciliary membrane; however, in *dpy-23(gm17)* mutants, OSM-9 also associated with an expanded far distal dendrite membrane and frequently formed punctate accumulations within this region (Figure 4A, C; Figure S3A). This expansion corresponds to the PCMC as it exists immediately proximal to the clearly definable and slender OSM-9-marked OLQ cilium structure. The punctate OSM-9 accumulations at the ciliary base of *dpy-23* mutants is frequently similar to that found in *bbs-8(nx77)* and *arl-13(tm2322)* mutants [29, 30], although an expanded PCMC was not observed in these animals (Figure S3B). Ciliary axonemal staining appeared grossly similar in both WT and *dpy-23(gm17)* mutants (Figure 4A and Figure S3A, B). Introduction of a transgene containing WT *dpy-23* rescued the OSM-9 mislocalisation defects (Figure 4C). In contrast to OSM-9, strong periciliary membrane localisation was also observed for GFP-tagged ODR-10 and SRBC-66 in WT cells, and this localisation was expanded in *dpy-23(e840)* mutants (Figure 4A; arrowheads; Figure S3C). Quantification of SRBC-66 signals revealed that the PCMC::cilium ratio was indeed increased in *dpy-23* mutants (Figure 4D and profiles in Figure S3D). This increase is not solely due to larger PCMC surface areas because signal intensities per unit area of periciliary membrane were also elevated in *dpy-23* worms, suggesting that SRBC-66 periciliary recycling is disrupted in these worms (Figure 4E and profiles in Figure S3E). Although a concomitant trend towards weaker SRBC-66 intensities per unit area of ciliary membrane was also observed in *dpy-23(e840)* worms (Figure 4E and Figures S3C, F), this phenotype did not present with strong statistical significance ($p=0.04$ in Figure 4E).

These data show that a number of ciliary transmembrane proteins are targeted to, and enriched at, the periciliary membrane of WT cells. Our findings also demonstrate a requirement for AP-2 in properly localizing OSM-9 and SRBC-66 between the ciliary and periciliary membrane compartments.

We also observed distinct and cell type-specific localisation defects of IFT proteins in *dpy-23* mutants. In WT amphid and phasmid channel cilia, IFT proteins localise along ciliary axonemes and form a small pool beneath the TZ at the distal-most end of the PCMC (Figure 4B, C; Figure S3G) [5]. However, in *dpy-23(e840)* mutants, OSM-6::GFP (IFT52) accumulated in the far distal dendrite region of phasmid neurons (Figure 4B, C; Figure S3G). This area of accumulation is consistent with the PCMC, as time-lapse imaging shows OSM-6-marked IFT particle activity immediately distal to this region (data not shown). Similarly, albeit to a lesser extent, OSM-3::GFP (KIF17) accumulated at the base of 13% of amphid cilia in *dpy-23* mutants, although in phasmid cilia, accumulation at the ciliary tips was observed (Figure 4B, C; Figure S3G). In contrast, PCMC accumulations were not typically observed for KAP-1 or BBS-7 (Figure 4B, C). Contrasting IFT protein localisation defects may reflect defects in turnaround phases of IFT, whereby in AP-2-disupted worms,

OSM-3 accumulates at the ciliary tips and OSM-6 at the ciliary base in phasmid neurons. A global defect in IFT turnaround is unlikely, as ciliary localisations of other IFT proteins, including XBX-1 (dynein light intermediate chain), were not affected (data not shown). Together, these results indicate that disruption of endocytic gene function affects the localisation of some but not all membrane and IFT proteins, and that differences are observed between different cilia subtypes.

Transport dynamics of ciliary proteins are affected in AP-2 disrupted worms

We next determined whether IFT was disrupted in endocytosis mutants. Most measurements were from amphid channel cilia, with a small minority (<10%) from phasmid cilia. Like previous observations [29], IFT proteins translocated anterogradely along middle segments of WT cilia at ~0.70 $\mu m.s^{-1}$ whereas OSM-3/KIF17 (but not KAP-1/kinesin-II) moved along WT distal segments at ~1.1–1.2 $\mu m.s^{-1}$ (Table 1; Figure S4A). However, in *dpy-23(e840)* middle segments, a subtle anterograde IFT rate defect was observed for OSM-3 (but not KAP-1, BBS-7 or OSM-6/IFT52), where this motor moved at ~ 0.84 $\mu m.s^{-1}$ (Table 1; Figure S4A). This was not caused by changes in OSM-3's intrinsic processivity, since in distal segments of *dpy-23* worms and middle segments of *dpy-23;klp-11* mutants (lacking kinesin-II motor activity), OSM-3 moved at its expected intrinsic speed of 1.2–1.3 $\mu m.s^{-1}$ (Table 1; Figure S4A). When rate distribution profiles were analyzed, ~20% of OSM-3 particles moved in *dpy-23* middle segments at speeds >1.1 $\mu m.s^{-1}$, whereas such fast moving particles were not observed in WT cilia (Figure S4A). OSM-3 retrograde rates appeared normal in *dpy-23* worms (1.13 ± 0.35 $\mu m.s^{-1}$; 29 particles/4 worms), compared with published observations (Table 1) [31, 32]. Together, these data suggest that in *dpy-23* mutant amphid channel middle segments, some fast moving (~1.1 $\mu m.s^{-1}$) OSM-3 motors are disengaged from slower moving (~0.7 $\mu m.s^{-1}$) OSM-3/kinesin-II/IFT assemblies, thereby raising average middle segment velocities for OSM-3. Accordingly, AP-2 may partially regulate docking of OSM-3 to middle segment anterograde IFT assemblies.

Since *dpy-23* worms possess short phasmid cilia (Figure 2A; Figure S2A), additional IFT assays were performed solely on these cilia. In contrast to the mostly amphid rates above, OSM-3 speeds were retarded in *dpy-23(e840)* phasmid middle segments (0.53 +/− 0.16 $\mu m.s^{-1}$; 66 particles/9 worms; $p<0.001$), compared to WT (0.74 +/− 0.14 $\mu m.s^{-1}$; 33 particles/4 worms). This could mean that in phasmid cilia, OSM-3 has reduced intrinsic velocity or is cargo for slow moving kinesin-II. Thus, OSM-3 is differentially regulated in amphid and phasmid channel cilia, demonstrating enhanced speeds in amphid cilia and reduced speeds in phasmid cilia.

Using fluorescence recovery after photobleaching, we also assessed whether endocytic genes regulate ODR-10 mobility within the AWB ciliary membrane. After photobleaching the distal portion of the ciliary signal, WT and *dpy-23* animals were found to possess similar signal recovery profiles and mobile fractions (Figure S4B). A normal ODR-10 recovery profile is consistent with *dpy-23* mutants possessing normal ODR-10 ciliary localisation (Figure 4A). Finally, we investigated whether endocytic components regulate the dendritic transport of ODR-10 and RAB-8-associated vesicles, which move bidirectionally along AWB dendrites to and from cilia [9, 10]. We observed significant but small increases in anterograde and retrograde dendritic velocities (Figure S4C).

Together, these data demonstrate modest and cell subtype-specific requirements for AP-2 complexes in regulating speeds of anterograde IFT and dendritic vesicle trafficking.

Sensory signaling and endocytosis may act in the same pathway to regulate AWB membrane area

The AWB ciliary membrane expansions of *dyn-1*, *rab-5* and AP-2 disrupted worms are similar to those previously described in mutants of signaling genes (*odr-1* receptor guanylyl cyclase, *tax-4* cyclic nucleotide-gated channel, *grk-2 G* protein-coupled receptor kinase) required for AWB sensory signal transduction [27]. Moreover, the expanded AWB ciliary membrane phenotypes in signaling mutants are suppressed by mutations in *bbs-8* and *rab-8* [27]. We asked whether sensory signaling defects underlie the endocytic gene-associated phenotype, or if these two groups of genes operate in distinct pathways, by analysing ciliary phenotypes of double mutants and comparing trafficking dynamics. We found that consistent with our previous report [27] nearly 100% of AWB cilia in *tax-4*, *grk-2* and *odr-1* single mutants exhibited increased membrane area; the penetrance of the phenotype was not altered in double mutant combinations with endocytic genes (Figure S5A, B). Similarly, the areas of AWB ciliary membrane expansion observed in sensory signaling mutants was not affected upon loss of endocytic gene function (Figure 5A). These data suggest that endocytosis and sensory signaling function in a common pathway, although we cannot rule out possible ceiling effects in the AWB ciliary membrane expansion phenotype.

To assess if these genetic relationships extend to cilia-related transport pathways, we determined whether transport dynamics of ciliary proteins were similarly affected in endocytosis and signaling mutants. Using the FRAP assay described above for ODR-10::GFP ciliary mobility, we found that *odr-1* mutants possessed modest increases in ODR-10 recovery compared to WT and *dpy-23* mutant worms (Figure S4B), suggesting that sensory signaling genes may partially regulate membrane protein dynamics within cilia. We also analysed dendritic trafficking of GFP::RAB-8 and ODR-10::GFP associated vesicles in AWB neurons and found that RAB-8 anterograde and retrograde velocities were somewhat reduced in *odr-1* mutants, whereas trafficking was unchanged for ODR-10::GFP (Figure S4C). This is in contrast to dendritic trafficking in *dpy-23* described above, where small increases in rates were found (Figure S4C). Thus, sensory signaling and endocytosis may differentially regulate trafficking of various proteins within AWB dendrites and cilia. Alternatively, the differing phenotypes could be indirect consequences of perturbing endocytic and sensory signaling gene functions.

In summary, endocytic and sensory signaling mutants have similar membranous AWB phenotypes, thus supporting a model that the corresponding genes function in the same pathway to modulate ciliary membrane volume.

DISCUSSION

Our results demonstrate a morphologically distinct periciliary membrane compartment (PCMC) at the base of nematode sensory cilia containing pools of endocytosis-associated proteins. We also observed clathrin at the base of human and *Chlamydomonas* flagella. These data expand previous findings of early endosomal proteins (RAB-5, STAM-1, HGRS-1) at the base of *C. elegans* male sensory cilia [18], clathrin coated pits and AP-2 complexes at the flagellar pocket of *Trypanosoma* and mammalian cells [17, 33–36], and clathrin, AP-2 mu and dynamin-related protein (DRP1) at *Tetrahymena* basal bodies [22]. Our observations also show functional requirements for endocytic genes in regulating metazoan periciliary and cilium morphologies. Indeed, in protists, the flagellar pocket is the major site of endocytosis and exocytosis [37].

Ciliary and periciliary membrane domains likely share common targeting properties for ciliary proteins since transmembrane SRBC-66 and ODR-10 localise to both membranes. These observations support the common view that at least some ciliary proteins (e.g.,

rhodopsin) are trafficked to cilia via vesicle fusion events at periciliary membranes [4, 38], thus providing pools of readily available proteins for cilia targeting.

Importantly, we show that endocytic genes regulate metazoan PCMC and ciliary membrane volume via a mechanism requiring *bbs-8* and *rab-8* gene function, and within a pathway that may include sensory signalling genes [27]. Indeed, a role for AP-2 directed endocytosis in regulating periciliary membrane homeostasis correlates well with previous findings for clathrin-mediated regulation of membrane volume at the flagellar pocket of *Trypanosoma* [39]. From our findings, we propose that ciliary membrane volume is maintained via tight regulation of membrane delivery via BBSome and RAB-8 proteins and membrane retrieval via AP-2-directed endocytosis (Fig. 5B). This model is supported by known roles for mammalian Rab8 in ciliary membrane extension and by biochemical associations of the BBSome with Rabin8, a guanosyl exchange factor for Rab8 [13]. Similar roles for endocytosis and exocytosis in regulating membrane homeostasis are described at the flagellar pocket of *Trypanosoma* and at the mammalian immune synapse [39, 40], suggesting this represents an efficient and conserved mechanism for regulating polarised membrane structure and dynamics.

Consistent with ciliary membrane abnormalities, ciliary protein localisation and transport were disrupted to varying degrees in endocytic gene-disrupted worms, suggesting endocytic events facilitate trafficking and recycling of some ciliary protein cargoes. Indeed, proteins frequently accumulated beneath AP-2-disrupted cilia implying that recycling events occur within the PCMC, which is consistent with the PCMC localisation of endocytic proteins. Indeed, our findings also correlate well with data showing *C. elegans* polycystins (PKD-2, LOV-1) accumulating at the ciliary base of *stam-1* mutants [18]. Although we were unable to directly visualise endocytosis in the PCMC, the clearly observable movement of RAB-5-associated particles within this compartment (Movie 1) likely reflects dynamic endomembrane transport.

Of note, PCMC and ciliary membrane expansions, as well as ciliary protein mislocalisation, were not observed in all ciliated cells following disruption of AP-2 complexes. For example, OSM-3/KIF17 accumulates at the PCMC and displays increased middle segment IFT velocities in amphid cells, whereas in phasmid cells, this motor accumulates at ciliary tips and undergoes reduced middle segment motility. A possible explanation is that different cell and cilia subtypes employ distinct mechanisms (e.g., clathrin dependent vs independent versions of endocytosis) to regulate ciliary membrane and protein transport, thus explaining why defects in cilia or the ciliary pocket were not observed in AP-2-depleted mammalian cells [17]. Indeed, for OSM-3 in phasmid cells, ciliary tip accumulation and reduced IFT were also found in *C. elegans dyf-5* MAP kinase mutants [41].

It would therefore be interesting to investigate if phasmid-specific effects on OSM-3 localisation and motility in AP-2 mutants occur via a *dyf-5* pathway. In conclusion, our findings uncover a role for *C. elegans* endocytic proteins at the ciliary base in regulating ciliary and periciliary membrane homeostasis, as well as efficient targeting of proteins to cilia. Correct regulation of these processes is likely critical for cilia and cell function, and may provide targets for developmental or activity-dependent pathways that sculpt cilia structures.

EXPERIMENTAL PROCEDURES

Worms were cultured, maintained and crossed via standard procedures. Fluorescent protein-tagged transgenes were generated using fusion PCR or via standard or Gateway cloning [42]. Transmission electron microscopy was performed as described [29]. Compound and

spinning disk confocal microscopy, equipped with EMCCD cameras, were employed to analyse cilium morphologies, IFT rates and dendritic transport. Time-lapse movies, still images and kymographs were generated using Andor iQ, SlideBook and ImageJ software. Additional experimental details are provided in Supplemental Information.

Supplementary Material

Refer to Web version on PubMed Central for supplementary material.

Acknowledgments

We thank *Caenorhabditis* Genetics Center, Japanese National BioResource Project, S. Shaham (Rockefeller University), X. Wang (National Institute of Biological Sciences, Beijing), B. Grant (Rutgers University) and E. Jorgensen (University of Utah) for strains and constructs. We also acknowledge S. Shaham for preliminary experimental data, and Dongshin Kim (Department of Physics, Brandeis University) for reagents. Some work was performed in the Laboratory of Sanford M. Simon at The Rockefeller University. Work funded by a Science Foundation Ireland President of Ireland Young Researcher Award (06/Y12/B928 to OEB), Seventh Framework Programme FP7/2009 (SYSCILIA grant agreement 241955 to OEB), NIH (R37 GM56223 to PS; T32 NS007292 to DD), NSF (MRI 0722582 to PS), and a postdoctoral PKD foundation fellowship (to DD).

References

1. Goetz SC, Anderson KV. The primary cilium: a signalling centre during vertebrate development. Nat Rev Genet. 2010; 11:331–344. [PubMed: 20395968]
2. Waters AM, Beales PL. Ciliopathies: an expanding disease spectrum. Pediatr Nephrol. 2011; 26:1039–1056. [PubMed: 21210154]
3. Silverman MA, Leroux MR. Intraflagellar transport and the generation of dynamic, structurally and functionally diverse cilia. Trends in cell biology. 2009; 19:306–316. [PubMed: 19560357]
4. Nachury MV, Seeley ES, Jin H. Trafficking to the ciliary membrane: how to get across the periciliary diffusion barrier? Annual review of cell and developmental biology. 2010; 26:59–87.
5. Williams CL, Li C, Kida K, Inglis PN, Mohan S, Semenec L, Bialas NJ, Stupay RM, Chen N, Blacque OE, et al. MKS and NPHP modules cooperate to establish basal body/transition zone membrane associations and ciliary gate function during ciliogenesis. The Journal of cell biology. 2011; 192:1023–1041. [PubMed: 21422230]
6. Blacque OE, Cevik S, Kaplan OI. Intraflagellar transport: from molecular characterisation to mechanism. Front Biosci. 2008; 13:2633–2652. [PubMed: 17981739]
7. Bae YK, Qin H, Knobel KM, Hu J, Rosenbaum JL, Barr MM. General and cell-type specific mechanisms target TRPP2/PKD-2 to cilia. Development (Cambridge, England). 2006; 133:3859–3870.
8. Deretic D, Huber LA, Ransom N, Mancini M, Simons K, Papermaster DS. rab8 in retinal photoreceptors may participate in rhodopsin transport and in rod outer segment disk morphogenesis. Journal of cell science. 1995; 108(Pt 1):215–224. [PubMed: 7738098]
9. Dwyer ND, Adler CE, Crump JG, L'Etoile ND, Bargmann CI. Polarized dendritic transport and the AP-1 mu1 clathrin adaptor UNC-101 localize odorant receptors to olfactory cilia. Neuron. 2001; 31:277–287. [PubMed: 11502258]
10. Kaplan OI, Molla-Herman A, Cevik S, Ghossoub R, Kida K, Kimura Y, Jenkins P, Martens JR, Setou M, Benmerah A, et al. The AP-1 clathrin adaptor facilitates cilium formation and functions with RAB-8 in C. elegans ciliary membrane transport. Journal of cell science. 2010; 123:3966–3977. [PubMed: 20980383]
11. Mazelova J, Astuto-Gribble L, Inoue H, Tam BM, Schonteich E, Prekeris R, Moritz OL, Randazzo PA, Deretic D. Ciliary targeting motif VxPx directs assembly of a trafficking module through Arf4. The EMBO journal. 2009; 28:183–192. [PubMed: 19153612]
12. Moritz OL, Tam BM, Hurd LL, Peranen J, Deretic D, Papermaster DS. Mutant rab8 Impairs docking and fusion of rhodopsin-bearing post-Golgi membranes and causes cell death of transgenic Xenopus rods. Mol Biol Cell. 2001; 12:2341–2351. [PubMed: 11514620]

13. Nachury MV, Loktev AV, Zhang Q, Westlake CJ, Peranen J, Merdes A, Slusarski DC, Scheller RH, Bazan JF, Sheffield VC, et al. A core complex of BBS proteins cooperates with the GTPase Rab8 to promote ciliary membrane biogenesis. Cell. 2007; 129:1201–1213. [PubMed: 17574030]
14. Das A, Guo W. Rabs and the exocyst in ciliogenesis, tubulogenesis and beyond. Trends in cell biology. 2011; 21:383–386. [PubMed: 21550243]
15. Westlake CJ, Baye LM, Nachury MV, Wright KJ, Ervin KE, Phu L, Chalouni C, Beck JS, Kirkpatrick DS, Slusarski DC, et al. Primary cilia membrane assembly is initiated by Rab11 and transport protein particle II (TRAPPII) complex-dependent trafficking of Rabin8 to the centrosome. Proceedings of the National Academy of Sciences of the United States of America. 2011; 108:2759–2764. [PubMed: 21273506]
16. Ghossoub R, Molla-Herman A, Bastin P, Benmerah A. The ciliary pocket: a once-forgotten membrane domain at the base of cilia. Biology of the cell / under the auspices of the European Cell Biology Organization. 2011; 103:131–144. [PubMed: 21275905]
17. Molla-Herman A, Ghossoub R, Blisnick T, Meunier A, Serres C, Silbermann F, Emmerson C, Romeo K, Bourdoncle P, Schmitt A, et al. The ciliary pocket: an endocytic membrane domain at the base of primary and motile cilia. Journal of cell science. 2010; 123:1785–1795. [PubMed: 20427320]
18. Hu J, Wittekind SG, Barr MM. STAM and Hrs down-regulate ciliary TRP receptors. Mol Biol Cell. 2007; 18:3277–3289. [PubMed: 17581863]
19. Inglis, PN.; Ou, G.; Leroux, MR.; Scholey, JM. WormBook. The C elegans Research Community. WormBook; 2007. The sensory cilia of C. elegans (March 8, 2007).
20. Correa JR, Atella GC, Menna-Barreto RS, Soares MJ. Clathrin in Trypanosoma cruzi: in silico gene identification, isolation, and localization of protein expression sites. J Eukaryot Microbiol. 2007; 54:297–302. [PubMed: 17552985]
21. Morgan GW, Allen CL, Jeffries TR, Hollinshead M, Field MC. Developmental and morphological regulation of clathrin-mediated endocytosis in Trypanosoma brucei. Journal of cell science. 2001; 114:2605–2615. [PubMed: 11683388]
22. Elde NC, Morgan G, Winey M, Sperling L, Turkewitz AP. Elucidation of clathrin-mediated endocytosis in tetrahymena reveals an evolutionarily convergent recruitment of dynamin. PLoS genetics. 2005; 1:e52. [PubMed: 16276403]
23. Gu M, Schuske K, Watanabe S, Liu Q, Baum P, Garriga G, Jorgensen EM. Mu2 adaptin facilitates but is not essential for synaptic vesicle recycling in Caenorhabditis elegans. The Journal of cell biology. 2008; 183:881–892. [PubMed: 19047463]
24. Esposito G, Di Schiavi E, Bergamasco C, Bazzicalupo P. Efficient and cell specific knock-down of gene function in targeted C. elegans neurons. Gene. 2007; 395:170–176. [PubMed: 17459615]
25. Sato M, Sato K, Liou W, Pant S, Harada A, Grant BD. Regulation of endocytic recycling by C. elegans Rab35 and its regulator RME-4, a coated-pit protein. The EMBO journal. 2008; 27:1183–1196. [PubMed: 18354496]
26. Starich TA, Herman RK, Kari CK, Yeh WH, Schackwitz WS, Schuyler MW, Collet J, Thomas JH, Riddle DL. Mutations affecting the chemosensory neurons of Caenorhabditis elegans. Genetics. 1995; 139:171–188. [PubMed: 7705621]
27. Mukhopadhyay S, Lu Y, Shaham S, Sengupta P. Sensory signaling-dependent remodeling of olfactory cilia architecture in C. elegans. Developmental cell. 2008; 14:762–774. [PubMed: 18477458]
28. Collet J, Spike CA, Lundquist EA, Shaw JE, Herman RK. Analysis of osm-6, a gene that affects sensory cilium structure and sensory neuron function in Caenorhabditis elegans. Genetics. 1998; 148:187–200. [PubMed: 9475731]
29. Cevik S, Hori Y, Kaplan OI, Kida K, Toivenon T, Foley-Fisher C, Cottell D, Katada T, Kontani K, Blacque OE. Joubert syndrome Arl13b functions at ciliary membranes and stabilizes protein transport in Caenorhabditis elegans. The Journal of cell biology. 2010; 188:953–969. [PubMed: 20231383]
30. Tan PL, Barr T, Inglis PN, Mitsuma N, Huang SM, Garcia-Gonzalez MA, Bradley BA, Coforio S, Albrecht PJ, Watnick T, et al. Loss of Bardet Biedl syndrome proteins causes defects in peripheral

sensory innervation and function. Proceedings of the National Academy of Sciences of the United States of America. 2007; 104:17524–17529. [PubMed: 17959775]

31. Qin H, Rosenbaum JL, Barr MM. An autosomal recessive polycystic kidney disease gene homolog is involved in intraflagellar transport in C. elegans ciliated sensory neurons. Curr Biol. 2001; 11:457–461. [PubMed: 11301258]
32. Snow JJ, Ou G, Gunnarson AL, Walker MR, Zhou HM, Brust-Mascher I, Scholey JM. Two anterograde intraflagellar transport motors cooperate to build sensory cilia on C. elegans neurons. Nature cell biology. 2004; 6:1109–1113.
33. Fonte VG, Searls RL, Hilfer SR. The relationship of cilia with cell division and differentiation. The Journal of cell biology. 1971; 49:226–229. [PubMed: 5555577]
34. Haycraft CJ, Banizs B, Aydin-Son Y, Zhang Q, Michaud EJ, Yoder BK. Gli2 and Gli3 localize to cilia and require the intraflagellar transport protein polaris for processing and function. PLoS genetics. 2005; 1:e53. [PubMed: 16254602]
35. Poole CA, Flint MH, Beaumont BW. Analysis of the morphology and function of primary cilia in connective tissues: a cellular cybernetic probe? Cell Motil. 1985; 5:175–193. [PubMed: 4005941]
36. Rattner JB, Sciore P, Ou Y, van der Hoorn FA, Lo IK. Primary cilia in fibroblast-like type B synoviocytes lie within a cilium pit: a site of endocytosis. Histol Histopathol. 2010; 25:865–875. [PubMed: 20503175]
37. Field MC, Carrington M. The trypanosome flagellar pocket. Nat Rev Microbiol. 2009; 7:775–786. [PubMed: 19806154]
38. Papermaster DS, Schneider BG, Besharse JC. Vesicular transport of newly synthesized opsin from the Golgi apparatus toward the rod outer segment. Ultrastructural immunocytochemical and autoradiographic evidence in Xenopus retinas. Invest Ophthalmol Vis Sci. 1985; 26:1386–1404. [PubMed: 2931395]
39. Allen CL, Goulding D, Field MC. Clathrin-mediated endocytosis is essential in Trypanosoma brucei. The EMBO journal. 2003; 22:4991–5002. [PubMed: 14517238]
40. Griffiths GM, Tsun A, Stinchcombe JC. The immunological synapse: a focal point for endocytosis and exocytosis. The Journal of cell biology. 2010; 189:399–406. [PubMed: 20439993]
41. Burghoorn J, Dekkers MP, Rademakers S, de Jong T, Willemsen R, Jansen G. Mutation of the MAP kinase DYF-5 affects docking and undocking of kinesin-2 motors and reduces their speed in the cilia of Caenorhabditis elegans. Proceedings of the National Academy of Sciences of the United States of America. 2007; 104:7157–7162. [PubMed: 17420466]
42. Hobert O. PCR fusion-based approach to create reporter gene constructs for expression analysis in transgenic C. elegans. BioTechniques. 2002; 32:728–730. [PubMed: 11962590]
43. Bacaj T, Lu Y, Shaham S. The conserved proteins CHE-12 and DYF-11 are required for sensory cilium function in Caenorhabditis elegans. Genetics. 2008; 178:989–1002. [PubMed: 18245347]
44. Dutcher SK, Morrissette NS, Preble AM, Rackley C, Stanga J. Epsilon-tubulin is an essential component of the centriole. Mol Biol Cell. 2002; 13:3859–3869. [PubMed: 12429830]

HIGHLIGHTS

- AP-2, clathrin, RAB-5 and dynamin localise at the base of *C. elegans* sensory cilia
- Ciliary and periciliary membrane is expanded in endocytosis gene-disrupted worms
- Ciliary membrane and IFT proteins mislocalise in AP-2-disrupted worms
- BBS-8 and RAB-8 are required for cilia membrane expansion in endocytic gene mutants

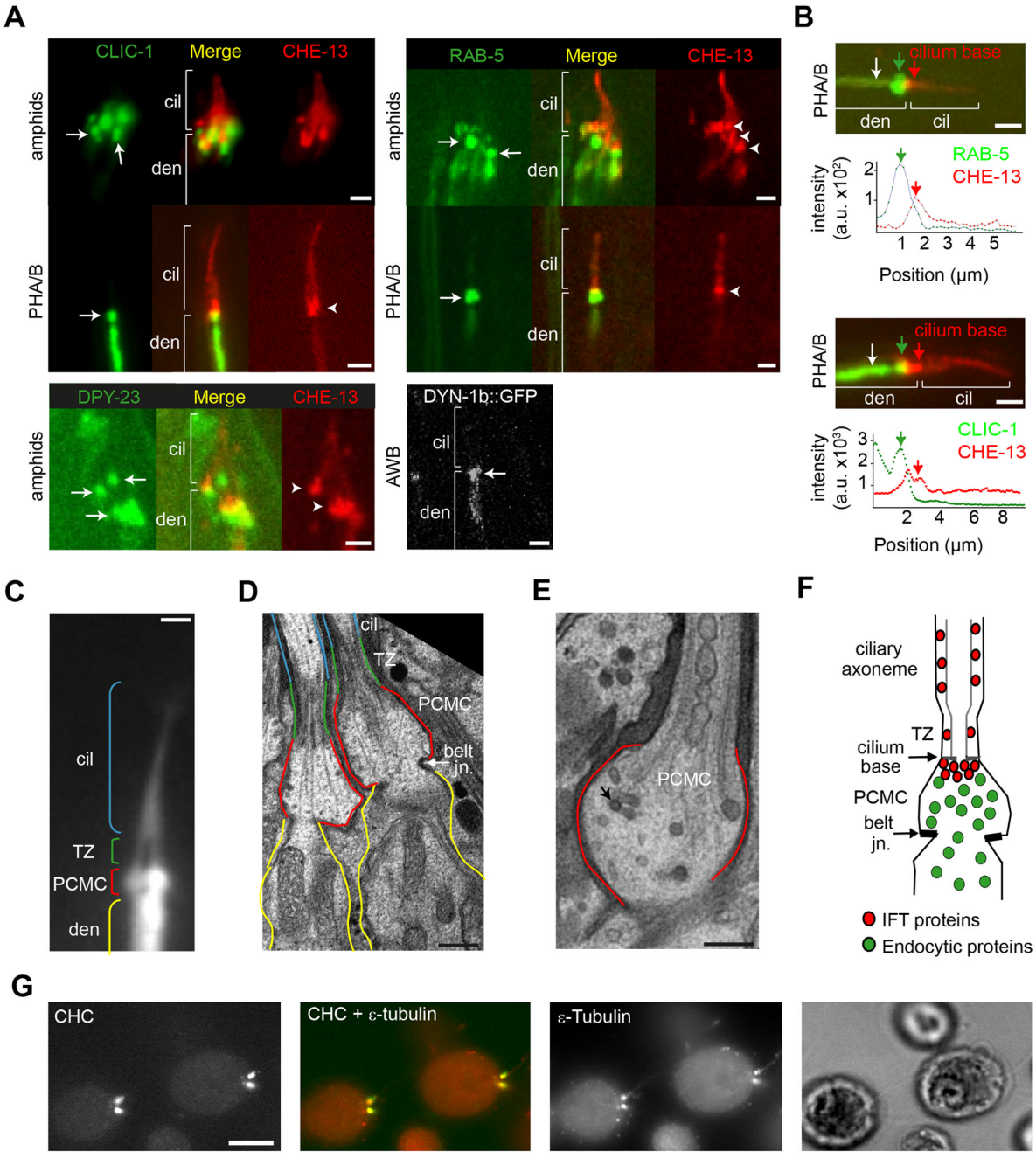

Figure 1. Localisations of *C. elegans* endocytosis-associated proteins overlap with a distinct compartment at the base of sensory cilia

(A) Co-localisation of indicated GFP-tagged endocytic proteins and mCherry-tagged CHE-13/IFT57 in multiple amphid or phasmid cilia. DYN-1 localisation is shown in the AWB olfactory cilium. GFP-tagged fusion genes were expressed under gene promoters active in ciliated cells, namely *che-12* (CLIC-1, CHE-13) [43], *arl-13* (RAB-5) [29], *rab-3* (DPY-23) [23] and *str-1* (DYN-1b) [27]. The *str-1*p*::dyn-1b::gfp* and *rab-3*p*::dpy-23::gfp* constructs are functional (Figure 2D, E, and Figure S2A, and ref [23]); functional assessment using phenotypic rescue could not be determined for *gfp::rab-5* and *clic-1::gfp*. Arrows; pools of accumulated endocytosis-associated protein near the ciliary base.

Arrowheads; pools of CHE-13::mCherry at the ciliary base. cil; cilia. den; dendrite. Scale bars; 2 μm. **(B)** Fluorescence intensity of CHE-13::mCherry relative to CLIC-1::GFP or GFP::RAB-5 indicating endocytosis-associated protein signals (green arrows) partly overlap with the IFT pool (red arrows). Data shown from one experiment. White arrows indicate starting position of measurements shown below each panel. Graphs aligned with fluorescence images. a.u.; arbitrary units. Scale bars; 2 μm. **(C)** PHA/B neuronal cilia in WT animals expressing the transcriptional PHA/B marker, *srb-6*p*::gfp*. cil; cilia. TZ; transition zone. den; dendrite. Scale bar; 1 μm **(D–E)** Low magnification (D; scale bar 500 nm) and high magnification (E; scale bar 200 nm) TEM images of longitudinal sections through ciliated amphid channel neurons. In D, cilia outlined in blue, TZ in green, far distal dendrite in red and more proximal dendrite in yellow. Belt junctions indicated in D. Black arrow in E denotes possible coated vesicle; other vesicles are unlabelled. **(F)** Schematic showing relative localisation of IFT and endocytic proteins within cilia and in the far distal dendrite pocket, which we call the periciliary membrane compartment (PCMC). TZ; transition zone. **(G)** *Chlamydomonas* clathrin heavy chain (CHC) colocalises with the centriolar basal body marker ε-tubulin [44] at the flagellar base. Scale bar; 5 μm.

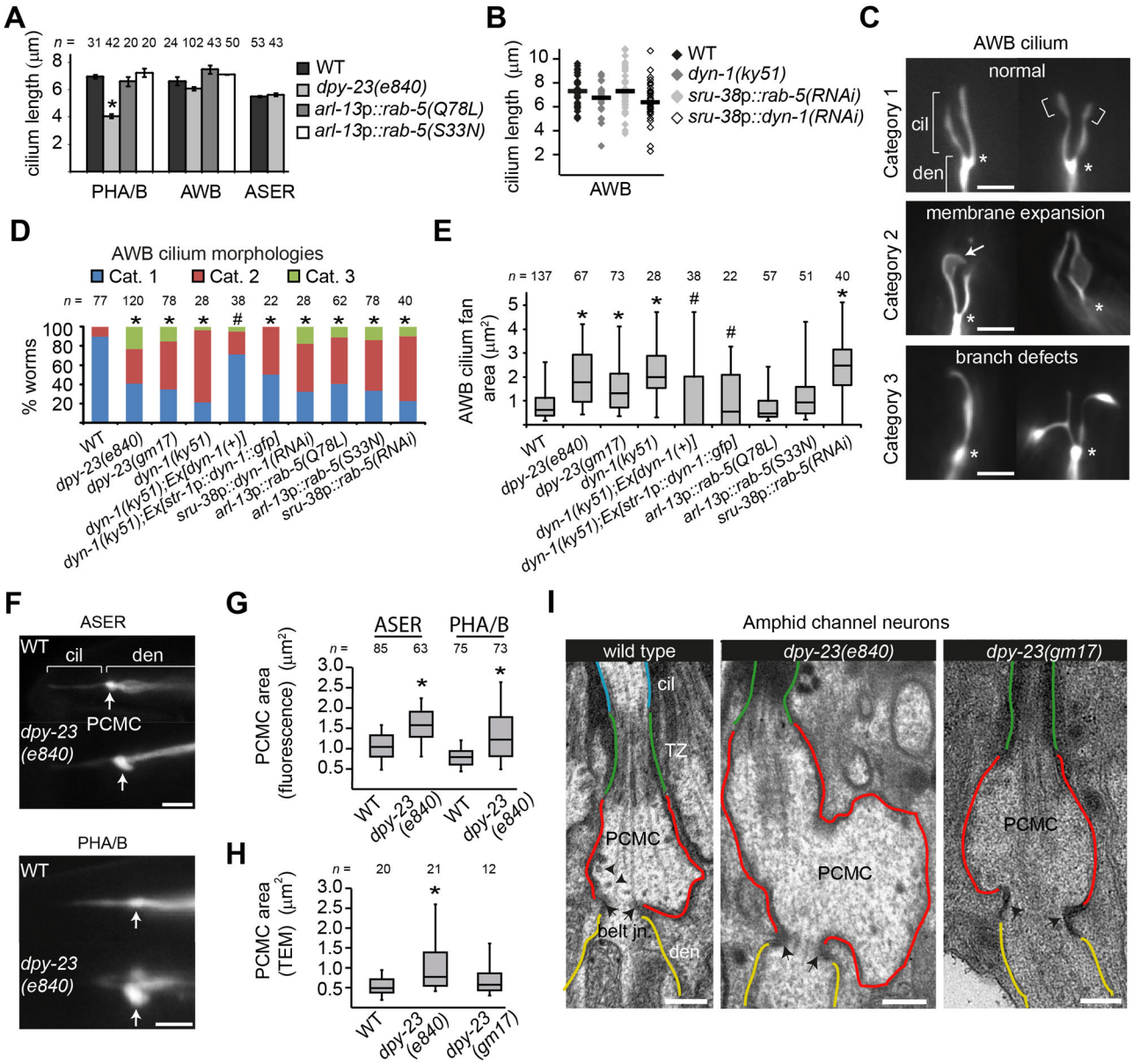

Figure 2. Disrupting endocytic gene function expands ciliary and PCMC membranes

(A, B) Quantification of cilium lengths in indicated genetic backgrounds. Cilia visualised using *osm-6/IFT52::gfp* (PHA/B cilia), *che-13/IFT57::mCherry* (PHA/B cilia; used in animals overexpressing N-terminal *gfp*-tagged *rab-5* variants), *str-1*p*::gfp* (AWB cilia) and *gcy-5*p*::gfp* (ASER cilia) reporters. >20 cilia analysed in B. Error bars; standard error of the mean. * p<0.001 compared with WT (one-way ANOVA followed by Dunnett's posthoc test). **(C)** Representative images of AWB cilium morphology categories. Asterisks denote base of cilia. Arrows denote expanded membrane or ectopic ciliary branches. Brackets indicate fans in WT cilia. Scale bars; 3 μm. **(D)** AWB cilia morphology phenotypes by category in the indicated genetic backgrounds. p<0.001 (cross-tabs and Chi-square test; compared with *WT or #*dyn-1(ky51)*). **(E)** Box and whisker distribution plots of AWB ciliary fan area measurements. Boxes; quartiles. Whiskers; 5th and 95th percentiles. * p<0.001 (non-parametric Mann-Whitney U test; comparison with WT values). # p<0.001

(non-parametric Mann-Whitney U test; comparison with *dyn-1(ky51)* values). **(F–I)** PCMC is enlarged in AP-2 disrupted worms.Shown in F are fluorescence images (scale bars; 3 μm) from WT and *dpy-23(e840)* worms expressing *srb-6*p*::gfp* (PHA/B) or *gcy-5*p*::gfp* (ASER) markers. Distribution of PCMC areas are shown as box and whisker plots in G. Shown in I are TEM images (scale bars; 300 nm) of longitudinal sections of amphid channel cilia from the indicated strains. Corresponding box and whisker plot distributions of PCMC areas from electron micrographs are shown in H. * $p<0.001$ (non-parametric Mann Whitney U test; compared with WT). Arrows in F denote PCMC, showing enlargement in *dpy-23* mutants. cil; cilium. TZ; transition zone. den; dendrite. *n*; number of cilia/PCMCs analysed.

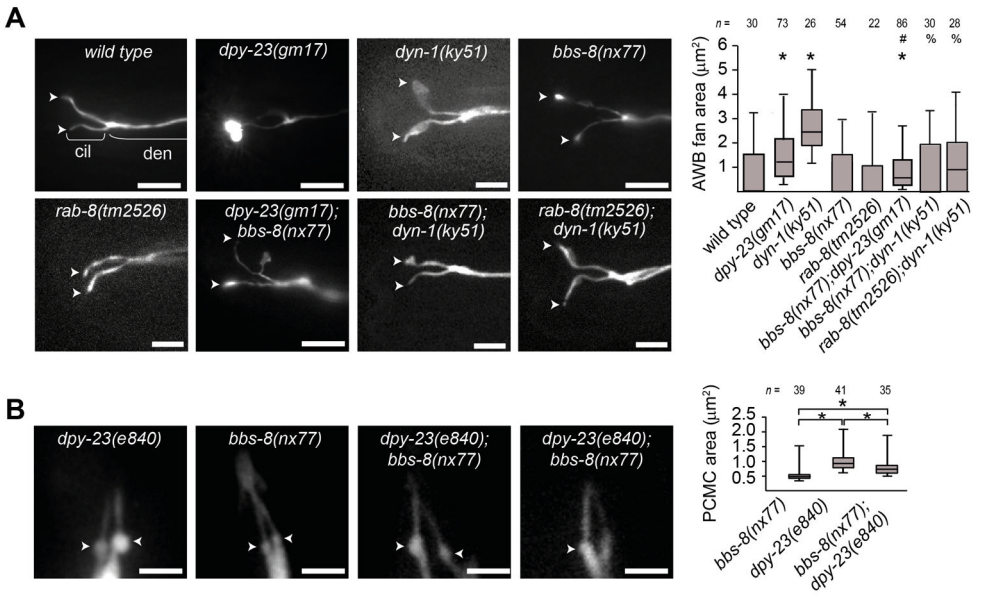

Figure 3. Genetic relationship between sensory signaling, *rab-8, bbs-8* and endocytic genes in regulating ciliary and PCMC membrane volume in AWB neurons

(A, B) Representative images and box and whisker plot distribution of AWB cilium fan areas (A) and PCMC areas in PHA/PHB (B) in the indicated genotypes expressing *str-1*p*::gfp* or *srb-6*p*::gfp* transgenes, respectively. For (A), p<0.005 (Mann-Whitney U test; compared with * WT, # *dpy-23(e840)*, or % *dyn-1(ky51)*). For (B), p<0.005 compared between indicated (*) genotypes (Mann-Whitney U test). Arrowheads in A; ciliary fans. Arrowheads in B; PCMC. Scale bars; 3 μm. cil; cilium. den; dendrite. *n*; number of cilia analysed.

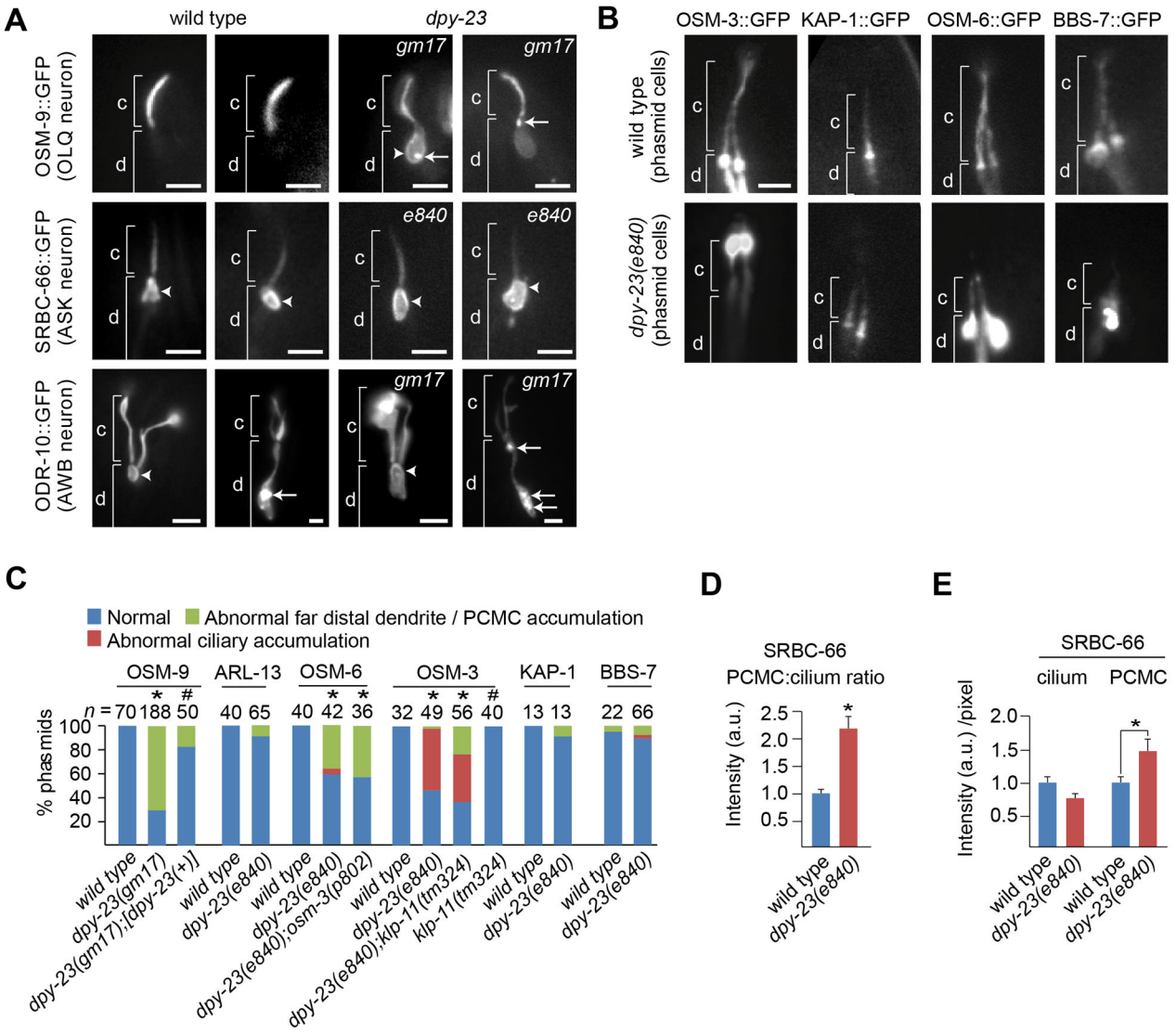

Figure 4. Differential requirements for AP-2 complexes in targeting transmembrane and IFT proteins to cilia

(A, B) Representative fluorescence images of cilia from animals expressing GFP-tagged proteins in the indicated neurons. c; ciliary axoneme, d; dendrite, Arrowhead; periciliary membrane. Arrows; punctate accumulations. scale bars; 2 μm. **(C)** Quantification of localisation phenotypes. * p<0.001 (cross-tabs and Chi-square test; compared with WT). # p<0.001 (cross-tabs and Chi-square test; compared with *dpy-23(e840)*). **(D, E)** Quantification of SRBC-66::GFP signal intensities in the PCMC and cilium of ASK neurons. Data acquired from images taken at identical exposure settings. All data normalized against WT values and data in E also adjusted for area. Each dataset comprises 39 measurements. a.u.; arbitrary units. Error bars; SEM. * p<0.001 (t-test; two-tailed).

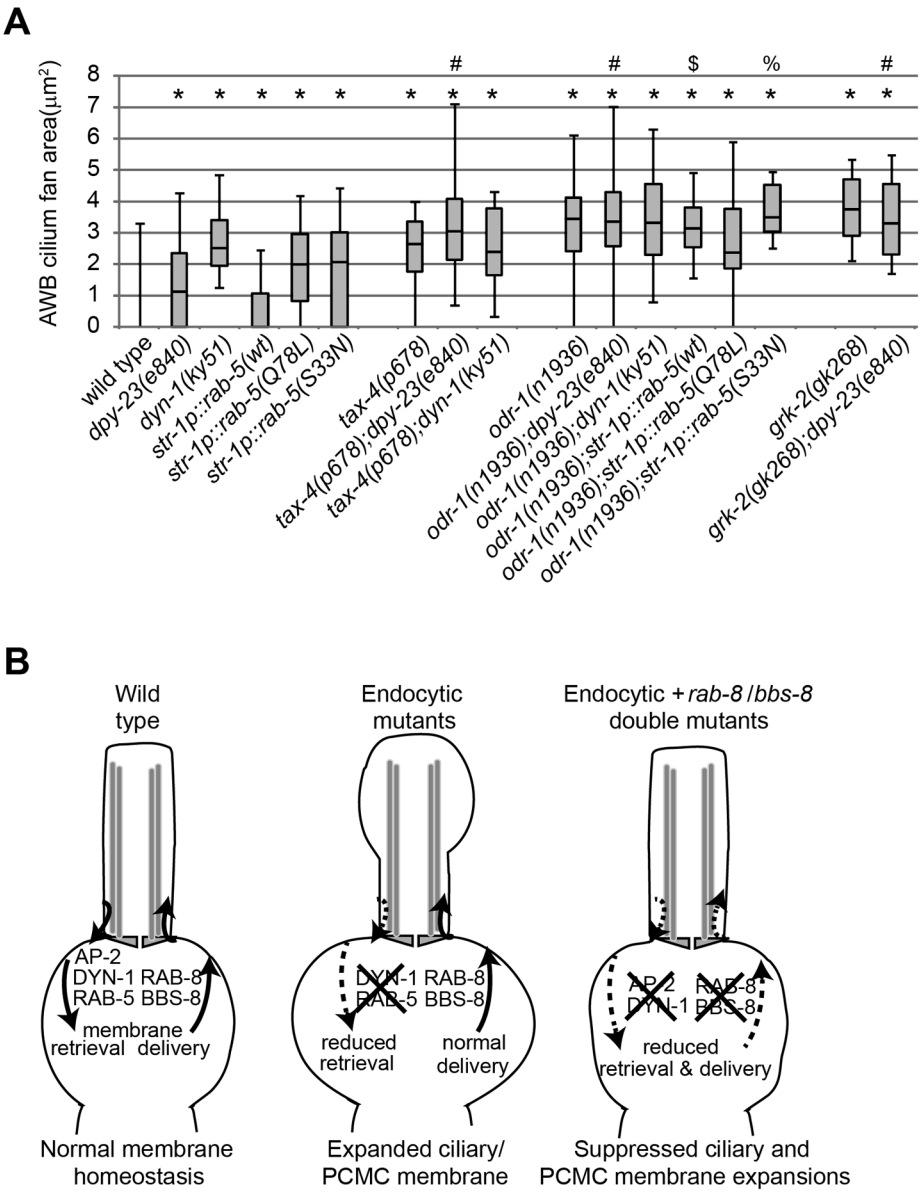

Figure 5. Sensory signaling may act in the same pathway as endocytic genes to modulate cilia membrane volume

(**A)** Analysis of PCMC areas in the indicated genotype expressing *str-1*p*::gfp*. All p-values <0.005 (Mann-Whitney U test) (compared with * WT, # *dpy-23(e840)*, $ *str-1*p*::rab-5(wt)* or % *str-1*p*::rab-5(S33N)*). **(B)** Model of *C. elegans* ciliary and PCMC membrane homeostasis. In WT worms, RAB-8 and BBS-8 facilitate addition of membrane to PCMC and ciliary regions, whereas endocytic AP-2, DYN-1 and RAB-5 facilitate retrieval of membrane, resulting in steady-state membrane volume at the PCMC and/or within the cilium. Membrane retrieval/addition is proposed to occur at the PCMC membrane. In endocytosis gene-disrupted worms, membrane retrieval is reduced relative to membrane delivery, thus membrane accumulates within cilia and the PCMC. This membrane accumulation/retrieval defect can be reversed by simultaneously disrupting membrane delivery via *rab-8* and *bbs-8* directed processes. Sensory signaling may act either upstream or downstream of endocytic genes.

Table 1

Anterograde velocities (μm.s^{-1}/standard deviation) of IFT proteins along amphid and phasmid channel cilia of WT, *dpy-23(e840)*, *klp-11(tm324)*, *klp-11(tm324);dpy-23(e840)*, *dpy-23(e840);osm-3(p802)* and *osm-3(p802)* worms.

		Middle segment			Distal segment			
IFT Protein	**Strain**	**Average**	**n/N**	**t test**	**Average**	**n/N**	**t test**	**No**
KAP-1::GFP	WT	0.69/0.11	119/12		none	none		3
	dpy-23	0.67/0.16	160/15	0.05	none	none		5
OSM-3::GFP	WT	0.71/0.14	428/25		1.17/0.21	103/8		3
	dpy-23	0.84/0.23	607/29	<0.001	1.12/0.21	143/15		6
	klp-11	1.2*	NA		1.2*	NA		NA
	klp-11;dpy-23	1.19/0.20	158/9		1.38/0.14	30/2		6
BBS-7::GFP	WT	0.70*	NA		1.11*	NA		NA
	dpy-23	0.70/0.08	425/32	0.23	1.19/0.23	116/12		6
OSM-6::GFP	WT	0.73/0.12	283/14		1.15/0.21	58/4		3
	dpy-23	0.65/0.16	322/20	p<0.001	0.96/0.29	145/14	<0.001	3
	dpy-23;osm-3	0.54/0.11	197/7					2
	osm-3	ND						

t-test; pairwise comparison with WT controls. n; number of particles. N; measured number of amphids and phasmids. ND; not determined. Asterisk; from Cevik *et al.* 2010 [29]. No: number of independent analyses. NA; not applicable.